

# **The Study of the Effects of Ion Chemical Activity on Conductivity of Poly(Dimethylsilylene-Co-Methylphenylsilylene)**

SHEHDEH JODEH

*Department of Chemistry, An-Najah National University, P.O. Box 7, Nablus, Palestine*

The effects of ion implantation on the electrical and structural properties of poly(dimethylsilylene-co-methylphenylsilylene), DMMPS, thin films have been investigated. Ionic species of krypton, arsenic, fluorine, chlorine, and sulfur were implanted at energies ranging from 35 to 200 keV and with doses of up to  $1 \times 10^{16}$  ion/cm<sup>2</sup>. The conductivity of the polymer increased, upon implantation, reaching a maximum value of  $9.6 \times 10^{-6}$  ( $\Omega\text{cm}$ )<sup>-1</sup> for the case of arsenic ion at a dose of  $1 \times 10^{16}$  ion/cm<sup>2</sup> and energy of 100 keV. The results showed that ion implantation induced conduction, in DMMPS, was primarily due to structural modifications of the material brought about by the energetic ions. Infrared analysis and Auger electron spectroscopy showed evidence for the formation of a silicon carbide-like structure upon implantation.

*Keywords:* implantation, conductivity, backscattering, thermal equilibrium, doping

## **INTRODUCTION**

Ion implantation has long been recognized as a vital technique for the introduction of dopant species in microelectronic device fabrication process. In this technique, a beam of dopant ions, accelerated through a potential, is

---

\*Corresponding Author: E-mail: sjodeh@hotmail.com; Fax: +972-9-2387982

allowed to impinge on the substrate surface. The highly energetic ions are slowed down by electronic and nuclear stopping mechanisms as they strike the surface of the substrate. The effects induced by implantation depend on the mass and energy of the ion, as well as, on the chemical and physical properties of the substrate [1,2,3,4]. Recently ion implantation has been successfully used in the modification of the electrical properties of organic compounds [5] and polymers [6]. Weber and coworkers [7] showed that the conductivity of polyacetylene increases on implantation with halogens. A larger increase in conductivity of up to 12 orders of magnitude was reported by Mazurek et al. [8] on implantation of polyphenylene sulfide (PPS) not only with the chemically active halogen ions but also with chemically inert ions such as krypton. Although the conductivities obtained by ion implantation were not as high as those obtained through chemical doping, the implanted polymers were stable in a normal environment with no measurable loss in the level of conductivity with time [8].

The implantation induced structural rearrangements are not limited to bond breaking and new bond formation but can also involve preferential removal of certain elements from the substrate. Lighter elements such as H<sub>2</sub> and volatile species are selectively depleted from the substrate on implantation [9]. This can lead to the production of novel thin film materials of useful electrical and optical properties.

Our overall objective in this area stems from our desire to formulate new thin film materials possessing useful electrical properties. In this study we have attempted to understand the effects of ion chemical activity on conductivity of poly(dimethylsilylene-co-methylphenylsilylene), (DMMPS). We chose this polymer because it possesses the following desirable properties: solution processibility, photo-conduction, thermal conversion to  $\beta$ -SiC and recent finding of electrical conduction properties on exposure to strong oxidizing agents [10].

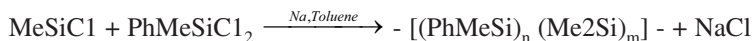
High energy (2 MeV) argon ion implantation of this polymer has been shown to produce a silicon rich material. The electrical conductivity after implantation was of the order of  $10^{-6}$  ( $\Omega$  cm)<sup>-1</sup> [9].

## EXPERIMENTAL

### Sample Preparation and Conductivity Measurements

Poly(dimethylsilylene-co-methylphenylsilylene), was synthesized by co-condensation of equimolar quantities of dimethyldichlorosilane and

methylphenylsilylane monomers in the presence of sodium suspension in dry toluene at 110 °C as given in the following equation [10]:



The reaction was conducted under a dry nitrogen atmosphere, and the polymer was precipitated by the addition of methanol. It was then dissolved in tetrahydrofuran and reprecipitated with methanol in order to remove the low molecular weight products.

The purified polymer was dissolved in toluene and was spin-coated on an interdigitated microelectrode. The electrode was similar to that reported by Mazurek et al. [5]. It was fabricated from aluminum interdigitated fingers (0.5 μm thick) on an oxidized silicon wafer. The electrode fingers, each with a width of 25 μm were separated by a distance of 25 μm. The thickness of the polymeric films were varied between 1200-5000 Å. The specific film thickness of each experiment was chosen to be slightly larger than the projected range of the implanted ion. The required thickness of each film was obtained by controlling the spinning speed, the time of spinning, and the concentration of the polymer solution. After spin coating, the polymer films were placed in a vacuum oven at 90 °C to evaporate the solvent.

The resistance measurements were carried out at room temperature under a dry nitrogen atmosphere in a shielded enclosure. The temperature dependence of conductivity was investigated using a polymer film coated on an oxidized silicon wafer. In this case, the two probe contacts were made at the surface of the film using an epoxy-silver compound.

### Ion Implantation and Sample Characterization

Polymer coated microelectrodes were ion implanted at room temperature. In all implantations, an ion beam having a current density of less than 0.8 μA/cm<sup>2</sup> was directed normal to the polymer film. The implanted ions were krypton, arsenic, chlorine, sulfur, and fluorine. These ions were chosen in order to study the effects of ion chemical activity on conductivity. The implantation parameters of the various ions are given in Table I. The depth profile parameters given in terms of the projected range, Rp, and range straggling, ΔRp (Table I) were calculated from the LSS theory [4].

The ion implanted films were characterized using ATR-FTIR spectrometry, Rutherford Backscattering (RBS), ESCA, and Auger electron spectroscopy. In these investigations, polymer films of thickness between 2000-

TABLE I  
Ion implantation parameters of DMMPS.

Ion	Ion Implantation Parameters of DMMPS					
	Energy	LSS		RBS		Approximate
	(keV)	R <sub>p</sub> (Å)	ΔR <sub>p</sub> (Å)	R <sub>p</sub> (Å)	ΔR <sub>p</sub> (Å)	Film Thickness (Å)
<sup>19</sup> F	35	1484	394			2000
<sup>19</sup> F	100	4331	987			5000
<sup>32</sup> S	100	2745	658			3500
<sup>35</sup> Cl	100	2588	624			3500
<sup>84</sup> Kr	100	1436	315	1268	420	2000
<sup>75</sup> As	100	1516	341	1436	380	2000
<sup>75</sup> As	50	840	192			1200
<sup>75</sup> As	150	2186	484			3000
<sup>75</sup> As	200	2962	622			3500

5000 Å were prepared by spin casting onto clean silicon wafers and then drying in a vacuum oven at 90°C for one hour.

Rutherford backscattering experiments were performed, using a 2.0 MeV Helium ion beam. The sample was tilted so that the He<sup>+</sup> beam was at an angle of 30° from the normal of the sample surface. RBS spectra of krypton and arsenic implanted samples were used to determine the depth profile parameters and compare them with those calculated from the LSS theory [1]. The parameters, R<sub>p</sub> and ΔR<sub>p</sub> were determined [11] from the RBS peak features of the implanted species (the energy shift of peak position and the full width at half height), and the energy loss factors for He<sup>+</sup> backscattered from the implanted ion in DMMPS. The energy loss factors were calculated from He<sup>+</sup> stopping cross section tables [11]. The calculated depth profile parameters are in a good agreement with those calculated from the LSS theory as shown in Table I. ATR-FTIR spectra of pristine and arsenic implanted (dose = 1 x 10<sup>16</sup> ion/cm<sup>2</sup>) samples were obtained using a Digilab FTS 20C FTIR spectrometer. ESCA and Auger electron spectroscopy of implanted samples were performed using a Physical Electronics Industries Model 549 ESCA/Auger Spectrometer. Depth profiles of the pristine and of the implanted samples were obtained by sputtering with a 2 keV argon ion beam.

TABLE 2  
Conductivities of ion implanted DMMPS.

Conductivities of Ion Implanted DMMPS		
Ion	Dose (ions/cm <sup>2</sup> )	$\sigma$ ( $\Omega\text{cm}$ ) <sup>-1</sup>
<sup>75</sup> As	1 x 10 <sup>16</sup>	9.6 x 10 <sup>-6</sup>
<sup>75</sup> As	1 x 10 <sup>16</sup>	2.2 x 10 <sup>-6</sup> (in plane)
<sup>75</sup> As	5 x 10 <sup>15</sup>	2.2 x 10 <sup>-6</sup>
<sup>75</sup> As	1 x 10 <sup>15</sup>	5.2 x 10 <sup>-9</sup>
<sup>84</sup> Kr	5 x 10 <sup>15</sup>	7.0 x 10 <sup>-6</sup>
<sup>35</sup> Cl	5 x 10 <sup>15</sup>	2.1 x 10 <sup>-6</sup>
<sup>32</sup> S	5 x 10 <sup>15</sup>	8.8 x 10 <sup>-7</sup>
<sup>19</sup> F	1 x 10 <sup>16</sup>	1.1 x 10 <sup>-6</sup>

## RESULTS AND DISCUSSION

The current-voltage (I-V) characteristics obtained at room temperature of ion implanted DMMPS showed ohmic behavior at voltages of less than 3 volts. Resistance values in this study were determined from the linear portion of the I-V curves. The corresponding conductivity values (given in Table II) were calculated using the relationship

$$l/\sigma = t(l/d)R$$

where  $\sigma$  is the conductivity in ( $\Omega\text{cm}$ )<sup>-1</sup>,  $l$  is the length of the electrode in cm,  $d$  is the distance between two electrode fingers,  $R$  is the measured resistance in ohm, and  $t$  is the thickness of the implanted region. As pointed out by Mazurek et al. [8] the largest contribution to the conductivity comes from a region in the film around the projected range, the region between

$R_p + \Delta R_p$  and  $R_p - \Delta R_p$ ; therefore,  $t$  is roughly equal to  $2 \Delta R_p$ . It is interesting to note that conductivity values obtained by surface resistivity measurements (in plane) were lower than those obtained using the microelec-

trode. Under identical implantation conditions, the surface resistivity of arsenic implanted DMMPS was lower by about a factor of four (see Table II). It should be noted, though, that variations of a factor of two in the conductivity values measured by using the microelectrodes were observed for samples implanted under similar conditions.

Table II shows that the maximum measured conductivity of  $9.6 \times 10^{-6} (\Omega\text{cm})^{-1}$ , was obtained with arsenic implantation at an ion dose of  $1 \times 10^{16}$  ion/cm<sup>2</sup>. At a dose of  $5 \times 10^{15}$  ion/cm<sup>2</sup>, krypton, which is chemically inactive caused a conductivity increase in DMMPS of a magnitude similar to that obtained by the more reactive arsenic ion at the same irradiation dose. These findings suggest that ion implantation induced conductivity in DMMPS is mainly due to molecular rearrangement caused by the energetic ions. The primary effect of the ion beam as it traverses the target material is the creation of highly energetic transient intermediates by ionization. In attaining the state of thermal equilibrium, a host of processes occur which include the dissociation of excited ions and molecules, internal conversion, and energy transfer, all of which result in more stable intermediates. The ultimate chemical changes observed on ion irradiation are primarily due to the chemical reactions which these reactive species undergo. Kaplan *et al.* [12] have shown from their work on ion irradiation of organic compounds that the factor determining the efficiency of ion induced rearrangements is the energy density in the track of the ion and not the total deposited energy. The greater the mass of the ion (at constant energy, dose rate, and dose) the higher is the energy density and the greater is the number of reactive intermediates produced. Thus for ions of comparable masses, as in the case of arsenic and krypton, equivalent levels of structural rearrangement are produced in the material giving rise to the observed similar conductivity values.

Implantation of fluorine, a chemically active ion but with a small ionic mass, was not as effective in raising the conductivity of DMMPS as the other implanted ions. The conductivity of the fluorine implanted sample was about one order of magnitude smaller than that of arsenic implantation at a constant dose but different ion energies (Table II). The choice of a 35 keV ion energy for fluorine implantation was made in order to obtain an ion range value,  $R_p$ , comparable to that of the arsenic ion implanted with an energy of 100 keV.

The data of Figure 1 indicate that the measured conductivity of ion implanted DMMPS is independent of the energy of the ion beam in the energy range of our experiments. Therefore, we attribute the low conductivity value in the case of fluorine to a lower bombardment induced disorder as a

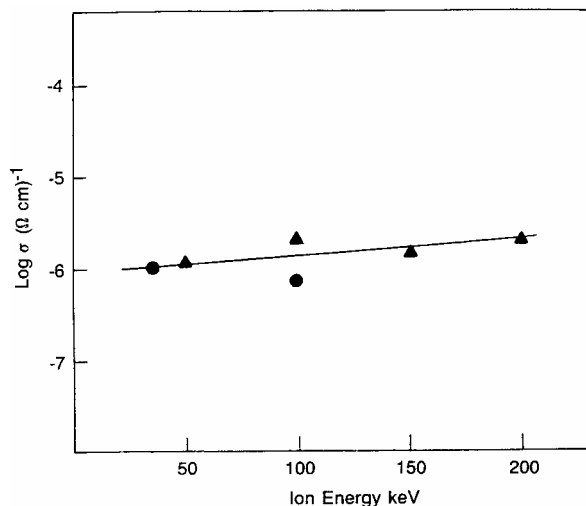


FIGURE 1

Ion energy-conductivity plot of arsenic at  $5 \times 10^{15}$  ion/cm<sup>2</sup> and fluorine at  $1 \times 10^{16}$  ion/cm<sup>2</sup> implanted DMMPS.

consequence of the small ionic mass of fluorine. It should be noted that recent studies on certain organic compounds and polymers [12,13] have shown that conductivities greater by a few orders of magnitude can be obtained with ion energies in the MeV ranges. This increase is due to the fact that at higher energies the magnitude of the energy loss of the ion is higher. In other words, at higher ion energies, more energy is deposited per ion causing greater molecular transformation in the material. Studies on high energy ion implantation of DMMPS with a 2 MeV argon ion have been recently reported by Venkatesan and coworkers [9]. Their measured conductivity value ( $<10^{-6}$  ( $\Omega\text{cm}^{-1}$ )), although slightly lower, is in the same range as those obtained in the present investigation. It appears that the ionic mass of the implanted species is the primary factor determining the level of conductivity in DMMPS, and that the energy of the ion plays no significant role in the process.

The implantation of chlorine and sulfur, which have comparable ionic masses, also yielded similar conductivities at a constant dose and ion energy (Table II). However, these average conductivity values are almost equal to that of arsenic implanted DMMPS (particularly in the case of chlorine) obtained under the same implantation conditions. Since the ionic mass of arsenic is twice as large as that of chlorine, the measured conductivity could

not be solely due to ion induced disorder in DMMPS. Unless there is some offsetting effects in the case of arsenic implantation, the high conductivity noticed in the case of chlorine and sulfur implantations is at least partly due to chemical doping by these two ions. In a similar experiment Mazurek *et al.* [8] concluded that the larger conductivity obtained at doses above  $1 \times 10^{16}$  ion/cm<sup>2</sup> in the case of bromine implantation of PPS as compared to those of arsenic and krypton ions was partly due to a chemical doping by the bromine.

Figure 2 shows the effect of dose on the measured conductivity of DMMPS implanted with arsenic at an energy of 100 keV. It can be seen that the conductivity level begins to saturate at a dose above  $5 \times 10^{15}$  ion/cm<sup>2</sup> suggesting that above this ion concentration level (at least for arsenic implantation) little bombardment induced rearrangement can be expected. These results are consistent with the data obtained on ion irradiated organic compounds [12] and polymers [8]. As indicated in Table II above, the highest conductivity obtained in DMMPS is that of arsenic implantation at a dose

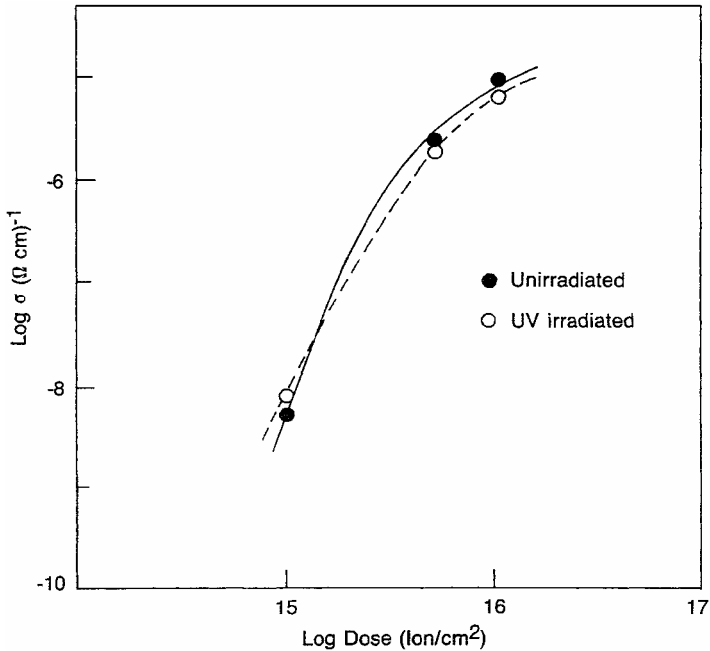


FIGURE 2  
Conductivity-ion dose relationship of arsenic implanted DMMPS at a 100 keV.

of  $1 \times 10^{16}$  ion/cm<sup>2</sup>. This value is more than an order of magnitude greater than that obtained by chemical doping of DMMPS with either AsF<sub>5</sub> or SbF<sub>5</sub> both of which are strong electron acceptors [10]. It is, however, five orders of magnitude lower than the conductivity of a sample of DMMPS cured (crosslinked) with UV irradiation and then doped with AsF<sub>5</sub> [10]. The nature of the effect of UV curing on the conductivity (or perhaps on the reaction of DMMPS with AsF<sub>5</sub>) of chemically doped DMMPS is unclear. It is known, however, that UV irradiation of this polymer in the solid state produces insoluble material [10]. It is also worth noting that ultraviolet treatment is utilized for maintaining the structural strength during the pyrolysis conversion of DMMPS to  $\beta$ -SiC at high temperatures. To determine if ultraviolet precuring can produce similar increases in the conductivity of ion implanted DMMPS, thin films were crosslinked by UV irradiation and then implanted with arsenic ions at various doses. The data plotted in Figure 2 indicate that, contrary to the case of chemical doping by AsF<sub>5</sub> UV precuring has little or no influence on the conductivity of ion implanted DMMPS. In this comparison the critical factor appears to be the chemical properties of AsF<sub>5</sub> (or SbF<sub>5</sub>) and the nature of its reaction with DMMPS. We now turn to the temperature dependence of conductivity of ion implanted DMMPS. It can be seen from Figure 3 that the conductivity of arsenic implanted DMMPS exhibits a thermally activated characteristic,  $\sigma\alpha e^{-E_a/kT}$ , with a change in the functional dependence around 60 °C. The activation energies obtained from the slope of  $\ln\sigma\alpha/T$  were 0.34 eV and 0.1 eV above and below 60 °C, respectively. Attempts to fit the data to the functions of variable range hopping mechanisms ( $\ln\sigma\alpha T^{-1/2}$  or  $\ln\sigma\alpha T^{-1/4}$ ) were not successful in the low temperature region (below 60°C). Above 60°C, the data fit the three functions  $T^{-1}$ ,  $T^{-1/2}$ , and  $T^{-1/4}$  equally well. Mazurek et al. [8] have observed a similar break in the  $\sigma\alpha/T$  curve for bromine and krypton irradiated PPS and have interpreted their data in terms of a phase transition. Thermal analysis of DMMPS showed a transition at 44°C which we attribute to the glass transition temperature of the polymer. As pointed out above, the change in the functional dependence of  $\sigma\alpha/T$  occurs around 60°C. This temperature, although 16 degrees higher, compares favorably with the measured glass transition temperature of DMMPS. The difference is not unexpected considering that the ion irradiated polymer is in a highly crosslinked state. It is well known that highly crosslinked polymers show higher transition temperatures than those of their uncrosslinked parents [11]. However, until we measure the thermal properties of ion implanted DMMPS, we are unable to state with certainty the reason for the observed change in the temperature dependence

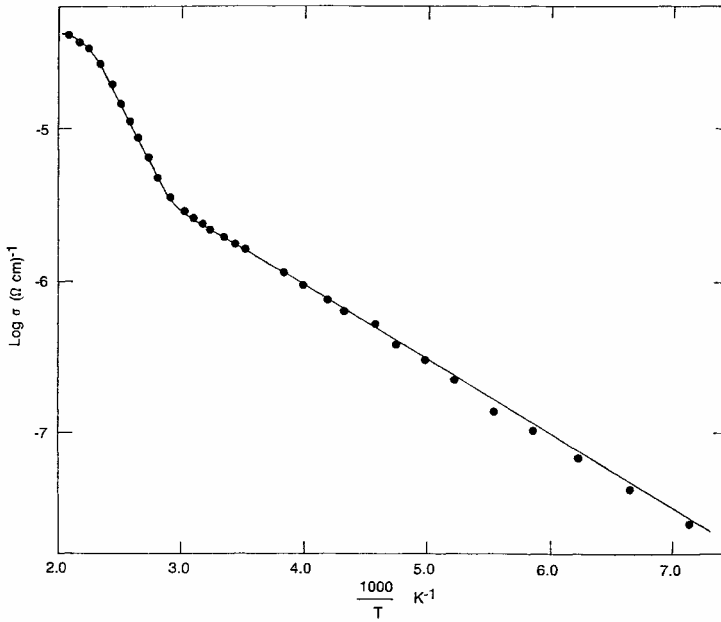


FIGURE 3  
Temperature dependence of conductivity of arsenic implanted DMMPS ( $1 \times 10^{15}$  ion/cm<sup>2</sup> at 100 keV).

of conductivity. On cooling the arsenic implanted DMMPS sample from 150 °C, no significant change in room temperature conductivity as observed. However, when the same sample was heated above 200 °C then cooled to room temperature, the conductivity (measured at room temperature) dropped by more than 50%. This can be attributed to annealing induced effects leading to, presumably irreversible chemical or structural changes in the material.

### Characterization of Implanted DMMPS

Rutherford backscattering spectra (RBS) of ion implanted DMMPS were obtained primarily to determine if the ions were indeed implanted in the polymer. Examples of such spectra are given in Figure 4 for krypton and chlorine implantations with a dose of  $5 \times 10^{15}$  ion/cm<sup>2</sup> and an ion energy of 100 keV.

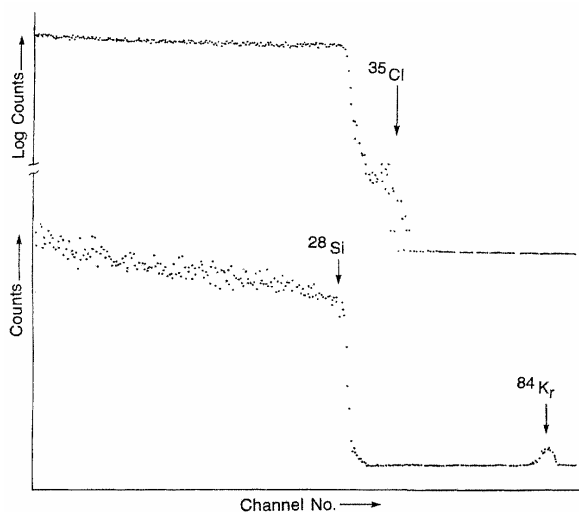


FIGURE 4  
Rutherford backscattering spectra of chlorine(top) and krypton(bottom) implanted DMMPS.

In these spectra the broad continuum is from the silicon of both the polymer and the substrate (Si). Elements of larger atomic masses such as the implanted krypton and chlorine appear at higher energy (channel number) than that of the silicon. A similar signal was also obtained for arsenic implantation. From these spectra the projected range,  $R_p$ , and the straggling,  $\Delta R_p$ , were calculated. As discussed in the experimental section, the results correlate reasonably well with the values of  $R_p$  and  $\Delta R_p$  obtained from LSS theory.

Additional information on the structural rearrangement induced by ion implantation in DMMPS was obtained from ESCA and Auger electron spectroscopy. Figure 5a shows the ESCA lines for pristine DMMPS. In addition to the  $C_{1s}$ ,  $Si_{2s}$ ,  $Si_{2p}$  and  $C_{KLL}$  lines, an oxygen 1s signal is also seen at a binding energy of 530 eV. This small oxygen signal is due to surface oxidation of DMMPS. An increase in the oxygen peak intensity was observed on implantation. The increase was greater in the case of the heavier arsenic ion (Figure 5c) than in the lighter fluorine ion (Figure 5b). Surface sputtering of these implanted samples resulted in a substantial reduction in the oxygen peak intensity. The highest oxygen concentration occurred near the surface of the irradiated film while at a depth near the projected range, the oxygen

concentration was insignificant. Therefore, it is more likely that the surface oxidation occurred after completion of the ion implantation. This type of oxidation is common in most organic polymer films exposed to high energy ion (or electron) beams and is due to the reaction of the generated free radicals and other reactive intermediates with atmospheric oxygen. Heavier elements (e.g., arsenic) cause a greater damage to the molecular structure (bond breaking) leading to a higher concentration of radicals available for reaction with oxygen. From the areas of the  $^{1s}$  signals, we estimated that at a dose of  $1 \times 10^{16}$  ion/cm $^2$  the surface oxygen content of the arsenic implanted sample was 45% greater than that of the fluorine implanted sample. It should be noted that all implanted samples showed surface oxidation the extent of which depended on the mass of the implanted ion.

Semi-quantitative elemental composition analysis (from peak areas) of pristine DMMPS gave a C:Si ratio of 4.5:1 as expected from the molecular

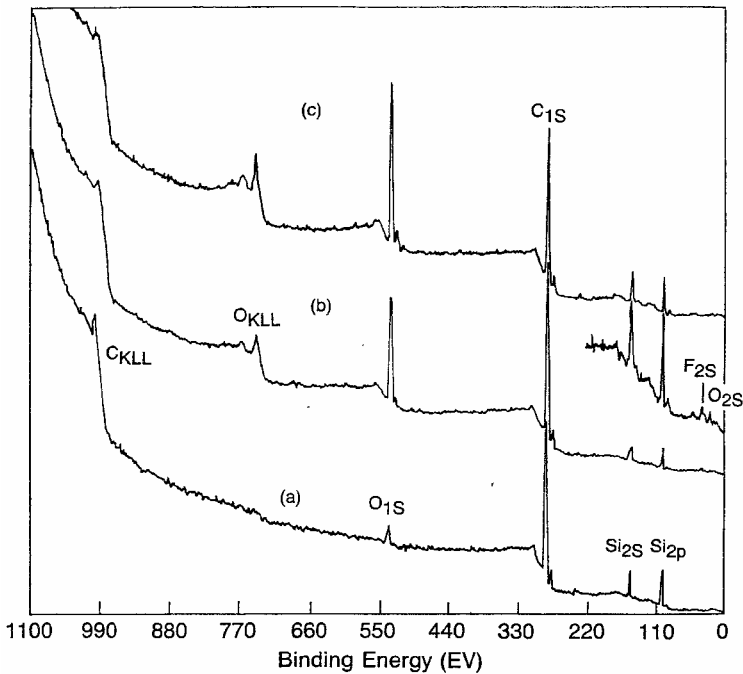


FIGURE 5  
ESCA spectra of DMMPS (a) pristine (b) fluorine implanted (c) arsenic implanted.

structure. A similar ratio was obtained for the arsenic implanted sample. Surprisingly, however, the fluorine implanted sample showed a C:Si ratio of 13:1 suggesting a substantial loss of silicon (or carbon enrichment) at the surface. Upon sputtering of the surface layer, a C:Si ratio of 4.5:1 was obtained. The origin of this variation in the surface composition of the fluorine implanted sample is not known; although surface contamination could not be ruled out.

Figure 6 shows the Auger spectra of pristine and arsenic implanted DMMPs. Whereas the unimplanted sample shows the polymer  $C_{KLL}$  (at 273 eV),  $Si_{LVV}$  at 88 eV and  $Si_{LLM}$  (at 1610 eV) electron signals only, the implanted sample displays an additional signal for the  $O_{KLL}$  Auger electron (at 510 eV) of the oxidized surface. The line shapes of Auger electron transitions have been used to gain information on the bonding nature of atoms in compounds. As reported by Haas et al, [12], the low energy side of the  $C_{KLL}$  Auger transition contains distinctive structures representative of the

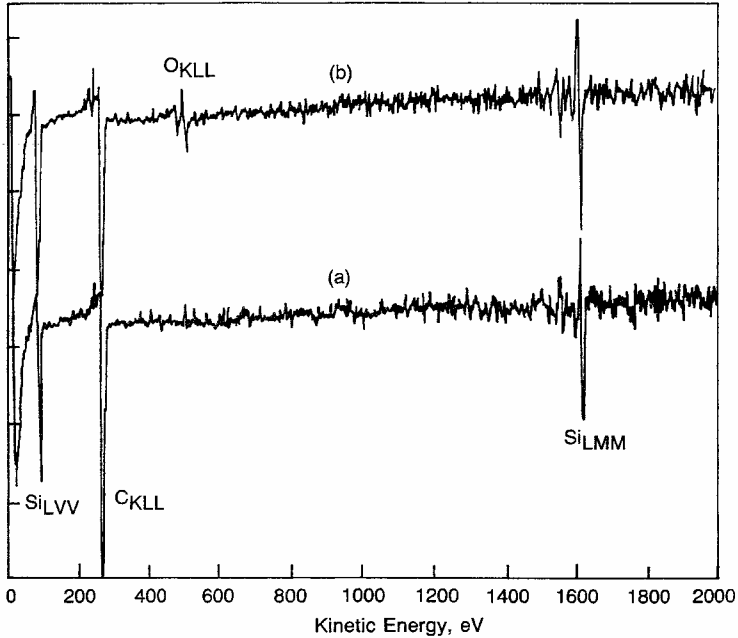


FIGURE 6  
Auger spectra of (a) pristine and (b) krypton implanted DMMPs.

chemical bonding of the carbon atoms in the substrate. Changes in carbon bonding as a result of ion implantation were indicated by the variation in the fine structure on the low energy side of the  $C_{KLL}$  transition. This is given in Figure 7 for krypton implanted DMMPS. The fine structure of the  $C_{KLL}$  transition obtained from the surface (Figure 7a) and that obtained after sputtering of a 400 Å layer (Figure 7b) are almost similar. Upon further sputtering to a depth of more than a 1000 Å the spectrum developed a detailed fine structure on the low kinetic energy side of the  $C_{KLL}$  transition (Figure 7c). These results indicate that the surface and the bulk carbons in ion implanted DMMPS exist in different bonding states. We suggest that this difference is due to ion implantation induced molecular rearrangement in the sample. Since the projected range of Kr ions in DMMPS is about 1400 Å at a 100 keV, substantially more ion induced damage exists at a depth of 1000 Å than at the surface. Haas and coworkers [15] have studied the change in the shape of the low energy side of  $C_{KLL}$  Auger transition with the change in the bonding nature of carbon composite including silicon carbide (Figure 7e). The similarity between the  $C_{KLL}$  line shape of silicon carbide and that of the sputtered

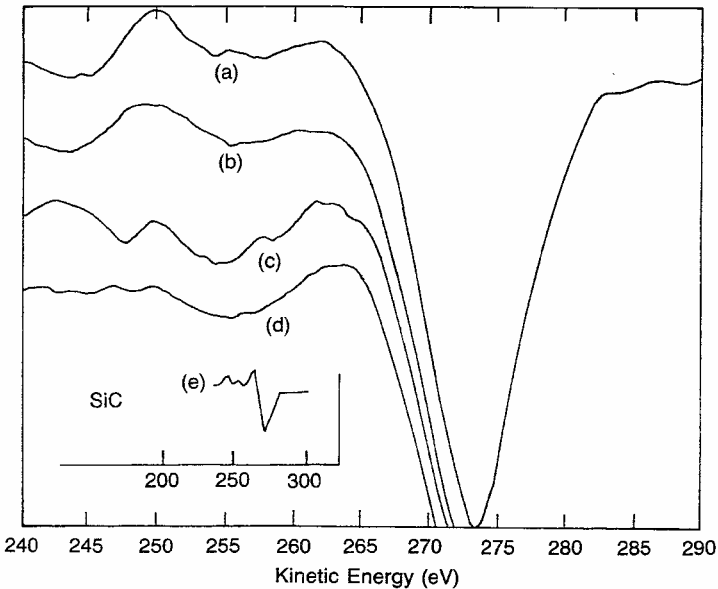


FIGURE 7  
Auger  $C_{KLL}$  signal of (a) surface of krypton implanted DMMPS (b) after sputtering of 400 Å, (c) after sputtering of a 1000 Å, (d) after sputtering of a 1000 Å but of unimplanted DMMPS, (e)  $C_{KLL}$  signal of silicon carbide (from Ref. 12).

(1000 Å) krypton implanted DMMPS indicates, presumably, a significant formation of a silicon carbide structure. Using a residual gas analyzer, Venkatesan and coworkers [9] showed that for a high energy (2 MeV) argon ion irradiation of DMMPS, the emitted gases consisted almost entirely of hydrogen with a very small amount of methane gas. Their Rutherford backscattering analysis showed a C:Si:H ratio of 7:2:1.38 in the implanted sample which indicates 0%, 20%, and 90% loss for Si, C, and H, respectively. In the present investigation the Auger compositional depth profile analysis by argon sputtering of ion implanted DMMPS revealed no change in the C:Si ratio. The depth profile of a 4000 Å thick DMMPS implanted with arsenic (100 keV) at a dose of  $1 \times 10^{16}$  ion/cm<sup>2</sup> is given in Figure 8. It can be seen that the C:Si ratio remains constant throughout the sample and that no significant change is apparent at Rp (1400 Å), the region at which most of the induced rearrangement is expected. It should be noted that sputtering with argon ion at an energy of 2 keV (used for depth profile) can, by itself, cause structural modifications of the material being analyzed. To determine whether the observed change in the C<sub>KLL</sub> line shape is in fact due

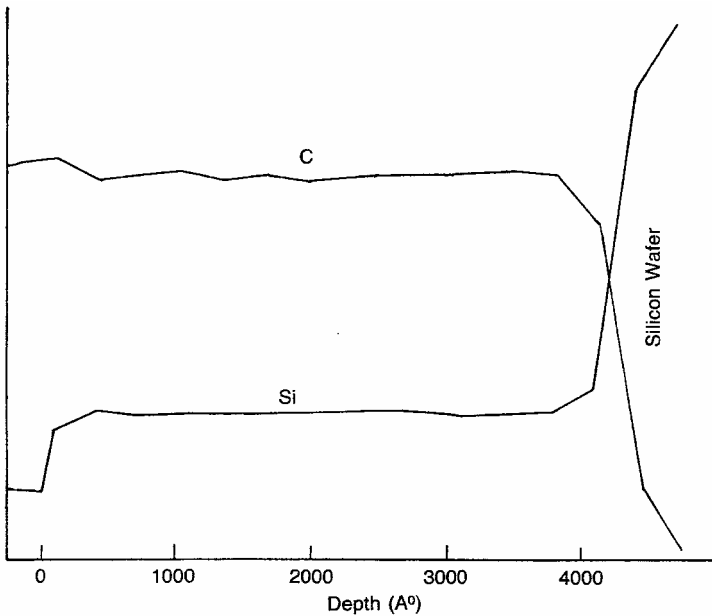


FIGURE 8  
Compositional depth profile of carbon and silicon in arsenic implanted DMMPS.

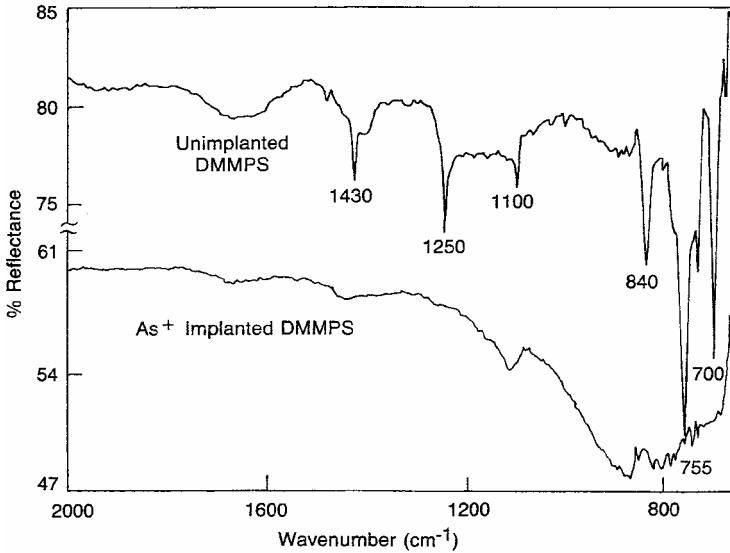


FIGURE 9  
Infrared multiple internal reflectance of unimplanted (top) and arsenic implanted DMMPS (bottom) at 100keV and  $1 \times 10^{16}$  ion/cm<sup>2</sup>.

to implantation, a pristine sample of DMMPS was sputtered to a depth of 1000 Å and the  $C_{KLL}$  spectrum was recorded (Figure 7d). Although the fine structure of the  $C_{KLL}$  transition of sputtered - pristine DMMPS is different from that of the sputtered-ion implanted sample, it is not identical to that of the surface

$C_{KLL}$  fine structure spectrum. It can, therefore, be concluded that the  $C_{KLL}$  spectrum of sputtered ion implanted DMMPS (Figure 7c) is most likely associated with rearrangements induced by both ion implantation and argon ion beam sputtering. It may be possible to minimize the sputtering induced effects by using low energy argon ion beams (e.g., 500 eV). However, this was not attempted.

Further evidence for the formation of a silicon carbide type structure in implanted DMMPS is obtained from ATR-FTIR spectrometry (Figure 9). The spectrum of the pristine film contains sharp bands corresponding to the various bonding vibrations of the polymer. These sharp bands disappeared on implantation, and a considerably different spectrum with a broad band around 800 cm<sup>-1</sup> was obtained. The broad structure at 800 cm<sup>-1</sup> is associated with Si-C stretching vibrations. The IR spectrum of SiC composite has a

broad band around  $800\text{ cm}^{-1}$  with no other major absorption [9]. These observations indicate a substantial loss of OH and aromatic structures and a significant SiC bonding formation in ion implanted DMMPS. The absorption at  $1110\text{ cm}^{-1}$  is associated with SiO or CO stretching vibrations resulting from the surface oxidation of the polymer. It is interesting to note that a similar IR spectrum was observed on irradiation of DMMPS with argon ions at an energy of

2 MeV [6], suggesting that the products from both high and low energy ion irradiations are fundamentally similar.

## CONCLUSIONS

Ion implantation of poly(dimethylsilylene-co-methylphenylsilylene), DMMPS, results in a semiconducting material, the conductivity of which depends primarily on the mass of the ion and the dose. The chemical nature of the ion appeared to play only a minor role in the level of conduction of the implanted product. Spectroscopic studies suggested that ion implantation caused major structural modification of DMMPS resulting in a material rich in SiC bonding structure.

## ACKNOWLEDGEMENT

The author wishes to acknowledge discussions and technical help from Prof. Hikmat S. Hilal, of Chemistry Department, ANU.

## REFERENCES

- [1] S. O. Kucheyev, J.S. Williams and I. T. Ferguson. (2002). *Appl. Phys. Lett.* **80**(5), 787 – 789.
- [2] O. Karabulut and B. G. Akinoglu. (2003). *Cryst. Res. Technol.* **38**(12), 1071-1076.
- [3] P. Lobotka and O. Chayka. (2004). *Phys. Stat. Sol.(A)*. **201**(7), 1493 – 1499.
- [4] 4. J. Linhard, M. Scharff, and H. E. Schiott, K. Danske, Vidensk. Selsk. (1963). *Mat. Fys. Medd.* **33**, 14.
- [5] S. R. Forrest, M. L. Kaplan, P. H. Schmidt, T. Venkatesan and A. J. Lovinger. (1982). *Appl. Phys. Lett.* **41**(8), 708.
- [6] M. S. Dresselhaus, B. Wasserman, and G. E. Wenk. (1984). *Mat. Res. Soc. Symp. Proc.* **27**, 413.
- [7] W. N. Allen, P. Brant, C. A. Carosella, J. J. DeCorpo, C. T. Ewing, F. A. Saalfeld and D. C. Weber, J. (1980). *Synth. Met.* **1**, 151.

- [8] H. Mazurek, D. R. Day, W. W. Maby, J. S. Abel, S. D. Senturia, M. S. Dresselhaus, and G. Dresselhaus. (1983). *J. Polym. Sci. Poly. Phys.*, ed. **21**, 537.
- [9] T. Venkatesan, T. Wolf, D. Allara, B. J. Wilkens and G. N. Tylor. (1984). *Mat. Res. Soc. Symp. Proc.* **27**, 439.
- [10] RR. West, L. D. David, P. I. Djurovich, K. L. Stearley, K. S. V. Srinivasan, and Hyuk Yu, J. (1981). *Am. Chem. Soc.* **103**,7352 .
- [11] W. K. Chu, J. W. Mayer and M. A. Nicolet, Backscattering Spectrometry. (1978) *Academic Press, New York, N.Y.*
- [12] M. L. Kaplan, S. R. Forrest, P. H. Schmidt, and T. Venkatesan. (1983). *J. Appl. Phys.* **55**(3), 732.
- [13] J. Bartko, B. O. Hall, and K. F. Schoch. (1986). *J. App. Phys.* **59**,1111.
- [14] K. Ueberreiter and G. J. Kanig. (1950). *J. Chem. Phys.* **18**, 399.
- [15] T. W. Haas, J. T. Grant, and G. J. Dooley III. (1972). *J. Appl. Phys.* **43**(4),1853.